



Cite this: *Polym. Chem.*, 2021, **12**, 2141

Ugi four-component polymerization of amino acid derivatives: a combinatorial tool for the design of polypeptoids†

Pierre Stiernet,^a Benoit Couturaud,^b Virginie Bertrand,^c Gauthier Eppe,^c Julien De Winter^d and Antoine Debuigne^{*a}

Polypeptoids, consisting of nitrogen-substituted analogues of polypeptides, have become a real asset in modern sciences especially in the biomedical field. To address the increasing demand for polypeptoid structures with specific properties, this work explores the combinatorial character of the Ugi-four component polymerization of amino acid derivatives such as dipeptides and aminobutyric acid compounds with different aldehydes and isocyanides. A library of structurally diverse polypeptoids is prepared accordingly. Thermal and solution properties of the latter are characterized and discussed in a structure–property relationship approach highlighting the impact of both the backbone and side chains. Some materials demonstrate pH-responsiveness, thermo-responsiveness with tunable transition temperatures and biocompatibility. Given the great variety of possible substrates and the promising properties of the obtained polypeptoids, this straightforward and combinatorial strategy is attractive for the future development of polypeptoids and resulting applications.

Received 25th January 2021

Accepted 8th March 2021

DOI: 10.1039/d1py00109d

rsc.li/polymers

Introduction

Polypeptoids are a class of non-natural biomimetic polymers that have raised huge interest in the last few years especially for biomedical applications.^{1–4} They consist of nitrogen-substituted analogues of natural polypeptides. In theory, the term polypeptoid should be restricted to polymers based on *N*-substituted glycine units⁵ but it is commonly used to designate indiscriminately all polypeptoid analogues, *i.e.* the *N*-substituted polyamide backbone, and so will it be throughout the text. The substitution of the nitrogen atom in polypeptoids accounts for major differences in their secondary and tertiary structures compared to polypeptides. While the secondary

structures of polypeptides are stabilized by hydrogen bonds between amides present in the backbone, the *N*-substitution prevents such interactions in polypeptoids. However, a wise choice of the *N*-substituted group can generate well-defined secondary structures similar to those of polypeptides by steric and electronic effects.^{1,6–14} These specificities generally impart to them good solubility in common solvents,^{15–17} high stability of their 3D structure¹⁸ and improved resistance to hydrolysis and proteolysis,^{4,19} phenomena that can be problematic for peptide-assisted drug delivery.^{19–22} Like polypeptides, polypeptoids exhibit good biocompatibility, a prerequisite for their applicability in the biomedical field.^{1,23,24}

The synthesis of polypeptoids can be achieved by various pathways.^{25–27} First, they can be prepared by classical iterative methods (Scheme 1A) involving repeated monomer addition/deprotection steps often carried out onto solid phase material^{28,29} or *via* a solid-phase submonomer approach based on primary amines and haloacetic acid building blocks which does not require the deprotection reaction.^{30,31} The iterative methods allow perfect sequence control with absolute monodispersity, but at the cost of a yield which decreases and a longer reaction time when the number of monomer units increases.²⁵ Alternatively, the living ring-opening polymerization (ROP) of *N*-substituted α -amino acid-*N*-carboxyanhydrides (NNCAs) gives access to poly- α -peptoids with high molar masses in good yields (Scheme 1B).^{1,2,23,32,33} This ROP has been successfully extended to β -NNCAs (Scheme 1B).³⁴

^aCenter for Education and Research on Macromolecules (CERM), CESAM Research Unit, Department of Chemistry, University of Liege (ULiege), Quartier Agora B6A, 13 Allée du Six Août, Sart-Tilman, 4000 Liège, Belgium.

E-mail: adebuigne@uliege.be

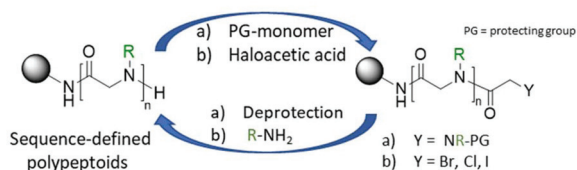
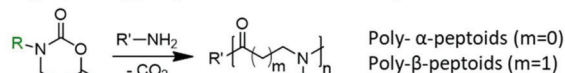
^bUniv Paris Est Creteil, CNRS, Institut de Chimie et des Matériaux Paris-Est (ICMPE), UMR 7182, 2-8 rue Henri Dunant, 94320 Thiais, France

^cMC²Lab – Laboratory of Mass Spectrometry, MolSys Research Unit, University of Liege (ULiege), Quartier Agora, 13 Allée du Six Août, Sart-Tilman, B-4000 Liège, Belgium

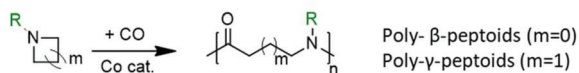
^dOrganic Synthesis and Mass Spectrometry Laboratory, University of Mons (UMons), 7000 Mons, Belgium

†Electronic supplementary information (ESI) available: Additional SEC, IR, NMR, MALDI, TGA, DSC and turbidimetry analyses. See DOI: 10.1039/d1py00109d

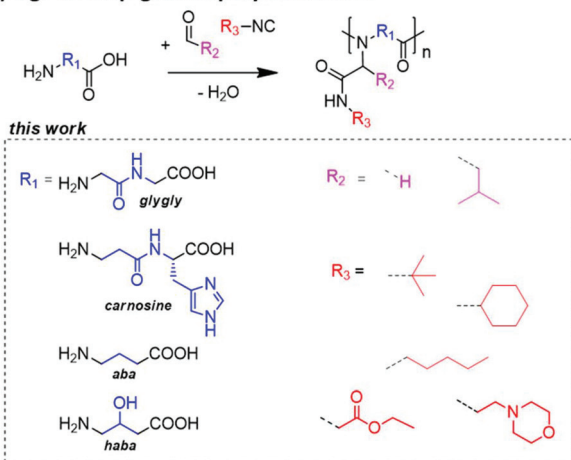
A) Iterative synthesis (a) monomer and (b) submonomer methods

B) Ring-opening polymerization of α and β -NNCAs

C) Cobalt-catalyzed carbonylative polymerization



D) Ugi-4C step-growth polymerization



Scheme 1 Synthesis methods of polypeptides and their analogues.

Although, the sequence regulation is more limited in this case, valuable polypeptoid structures including statistical and block copolymers can be produced accordingly.³³ As a downside, the synthesis of NNCA is not trivial especially when the complexity of the side chains increases. Moreover, their ROP must be carried out under strict anaerobic and anhydrous conditions due to the moisture sensitivity of these monomers. Note that the synthesis of poly- β -peptoids and poly- γ -peptoids can also be achieved by ring opening copolymerization of aziridine and azetidine with carbon monoxide (Scheme 1C).^{17,35} Another recent strategy for preparing polypeptoid analogues relies on the Ugi four-component reaction (Ugi-4CR) (Scheme 1D). This efficient, atom-economical, catalyst-free and air-tolerant multicomponent reaction (MCR) occurs under mild conditions and generates α -amido amide derivatives in one pot from carbonyl, amine, carboxylic acid and isocyanide reactants.³⁶ The key steps consist of the condensation of the carbonyl and the amine to afford the formation of iminium that undergoes a nucleophilic attack from the isocyanide to form a nitrilium intermediate. Eventually, after the addition of carboxylate onto the nitrilium, an α -amido amide is generated

through acyl group migration (Mumm rearrangement) with water as the sole by-product (Fig. S1A†).³⁷ Since its introduction in macromolecular chemistry by Meier *et al.*,³⁸ the Ugi-4CR has been applied to several monomers giving access to a large variety of amide-containing polymers^{39–41} including polypeptoid analogues (Scheme 1D).⁴² Sequence-defined polypeptoids were produced by the Ugi-4CR through an iterative approach^{43,44} whereas the step-growth process based on the Ugi-4CR paved the way to sequence-undefined polypeptoids.^{24,42,45–48} For example, lysine methyl ester and *N*-*boc*-glutamic acid served as AA and BB type monomers in the Ugi-4C step-growth polymerization leading to alternating polypeptoids and the corresponding polyampholytes upon cleavage of the protecting groups.²⁴ Some alternating polypeptide-*alt*-peptoids were also produced by the Ugi-4CR involving a carboxylic acid/isocyanide AB monomer and an imine.^{47–49} In this context, amino acid derivatives possessing two of the four functions necessary for the Ugi-4CR quickly drew attention as natural AB building blocks. Unfortunately, the use of α -amino acids is hampered by a side-reaction consisting of intramolecular cyclisation *via* the Ugi-4CR leading to oxazepinone (Fig. S1B†).⁴⁵ This can be tackled by increasing the distance between the amine and the carboxylic acid in the building block which limits this side reaction and allows the step-growth polymerization to occur. For example, a modified lysine (*N* α -*Boc*-L-lysine), with α -amine protected by a *tert*-butoxycarbonyl group and a free ϵ -amine, led to the corresponding poly- ϵ -peptoids by reaction with an isocyanide and a carbonyl derivative.⁴⁵ Poly- γ - and poly- δ -peptoids were prepared following the same strategy.⁴⁵ Finally, some alternating poly(peptides-*alt*-peptoids) have also been synthesized by Ugi-4 component polymerization (Ugi-4CP) of simple dipeptides carried out in water in the presence of *tert*-butyl isocyanide and formaldehyde.⁴⁶

In this work, we explored the combinatorial character of the Ugi-4CR in the step-growth polymerization of a variety of amino acid derivatives, isocyanides and aldehydes, in order to access structurally diverse polypeptoids with specific properties and fulfill the ever-growing demand for unique polypeptoid materials (Scheme 1D). In addition to simple dipeptides like glycylglycine, we considered β -alanyl-L-histidine as a difunctional substrate as well as some easily available 4-amino-butyric acid compounds with different polarities. These building blocks were reacted with common aldehydes, namely formaldehyde and isobutyraldehyde, in combination with various isocyanides bearing differently substituted aliphatic groups or hydrophilic substituents such as the morpholino function. This systematic study notably emphasized the impact of the solvent choice on the reaction efficiency and thus on the molar mass of the polymers. A library of unprecedented polypeptoids was prepared accordingly. The thermal properties and solution behaviors of the latter were then characterized and discussed in a structure–property relationship approach. Some of them exhibit pH sensitivity but also thermoresponsiveness with tunable transition temperatures. The biocompatibility of novel water-soluble polypeptoid structures was also validated by cell viability tests.

Experimental section

Materials

tert-Butyl isocyanide (*t*BuNC) (98%), cyclohexyl isocyanide (98%), 1-pentyl isocyanide (97%) and formaldehyde (37 wt% in H₂O) were purchased from Sigma-Aldrich, γ -aminobutyric acid (>99%), 2-morpholinoethyl isocyanide (>98%), ethyl isocyanacetate (95%), glycyglycine (>99%) and isobutyraldehyde (>99%) were purchased from Acros Organics and 4-amino-3-hydroxybutyric acid (>98%) was purchased from Tokyo Chemical Industry Europe (TCI). Beta-alanyl-L-histidine (98%) was purchased from abcr and dimethylformamide (DMF) and diethylether (Et₂O) were purchased from VWR Chemicals. Methanol (MeOH) was purchased from Fisher Chemical. All chemicals and solvents were used without purification. Spectra/Por® dialysis tubings (cut-off, 1 kDa) were purchased from SpectrumLabs. DMEM solution: 89% Dulbecco's Modified Eagle's Medium, high glucose (4.5 g L⁻¹ D-glucose), GlutaMAX™ Supplement, pyruvate (Gibco, Grand Island, NY, United States), 10% fetal bovine serum (Gibco, Grand Island, NY, United States), and 1% of antibiotics (penicillin/streptomycin 10 000 U/10 000 μ g ml⁻¹) (Lonza, Basel, Switzerland). DMEM/F-12 no phenol red (Gibco, Grand Island, NY, United States) and CellTiter 96® Aqueous One Solution Cell Proliferation Assay (MTS) (Promega, Leiden, The Netherlands) were obtained.

Characterization

Molar masses (M_n , M_w) and dispersity (D) of the polymers were characterized by size exclusion chromatography (SEC) at 55 °C in dimethylformamide (DMF) containing LiBr (0.025 M) using a flow rate of 1 mL min⁻¹ with polystyrene calibration. SEC curves were recorded with a Waters chromatograph equipped with two columns (Waters Styragel pss gram 100 Å (x2)) in an oven at 55 °C and a refractive index detector (Waters 2414) working at 40 °C. ¹H NMR, HSQC and COSY spectra were recorded at 298 K with a Bruker Avance III HD spectrometer ($B_0 = 9.04$ T) (400 MHz) and treated with MestReNova software. IR spectra were recorded on a Thermo Fisher Scientific Nicolet IS5 system equipped with an ATR ID5 module using a diamond crystal (650 cm⁻¹–4000 cm⁻¹). Differential scanning calorimetry (DSC) was performed on a TA Instruments Q1000 DSC system, using hermetic aluminium pans, indium standard for calibration, nitrogen as the purge gas, and a sample weight of ~5 mg. The sample was cooled down to -80 °C at a 20 °C min⁻¹ cooling rate, followed by an isotherm at -80 °C for 2 min and heating up to 180 °C at a 10 °C min⁻¹ heating rate. These cycles were repeated twice. The fourth cycle (last heating from -80 to 180 °C) was analysed. Thermogravimetric analyses (TGA) were carried out with a TGA 2 large furnace from Mettler Toledo under nitrogen at a heating rate of 20 °C min⁻¹ from ambient temperature to 600 °C with a sample weight of ~10 mg. Turbidity was determined by measuring the absorbance at 260 nm on a Jasco v-630 spectrophotometer. The polymers (P₁, P₂, P₃, P₅ and P₁₀) were dissolved in Milli-Q water (2 mg mL⁻¹) and subjected to heating-cooling cycles in

a quartz cuvette at a constant rate of 2 °C min⁻¹ in a temperature controlled multicell holder. pH measurements were performed on a pH/ORP meter HANNA HI2211. The calibration of the instrument was performed with HANNA buffer solutions at pH 7.01 and 4.01 before the titrations. Regarding the viability of HeLa cells, the CellTiter 96® Aqueous One Solution Cell Proliferation Assay is based on similar principles to the widely used MTT assay. The active component is a tetrazolium compound called MTS (similar to MTT and its derivatives), which is reduced to a coloured formazan product. The amount of the formazan product is directly proportional to the number of living cells; therefore, cell proliferation or death can be quantified by reading the plate at 490 nm. The absorbance was read at 490 nm using a Powerwave X microplate spectrophotometer (BioTek Instruments Inc., Winooski, USA) and the viability was calculated and normalized from the absorbance of control samples taken as 100% (PS).

The Matrix-Assisted Laser Desorption/Ionization Time-of-Flight (MALDI-ToF) mass spectra were recorded using a Waters QToF Premier mass spectrometer equipped with a Nd:YAG laser using the 3rd harmonic with a wavelength of 355 nm. In the context of this study, a maximum output of ~65 μ J is delivered to the sample in 2.2 ns pulses at a 50 Hz repeating rate. Time-of-flight mass analyses were performed in the reflection mode at a resolution of about 10 000. *trans*-2-(3-(4-*tert*-Butylphenyl)-2-methyl-2-propenylidene)malononitrile (DCTB) was used as the matrix and was prepared as a 40 mg mL⁻¹ solution in chloroform. The matrix solution (1 μ L) was applied to a stainless steel target and air-dried. Polymer samples were dissolved in adequate solvent to obtain 1 mg mL⁻¹ solutions and 20 μ L of NaI solution (2 mg mL⁻¹ in acetonitrile) were added as the source of a cationization agent. Then, 1 μ L aliquots of these solutions were applied onto the target area (already bearing the matrix crystals) and then air-dried.

General procedure for Ugi-4C polymerization

In a typical experiment, the amino acid (1.0 mmol) was dissolved in 0.62 mL of Milli-Q H₂O, MeOH or a H₂O/MeOH mixture (1:1 v:v). Aldehyde (1.3 mmol) was added to the stirred solution at room temperature followed by addition of isocyanide (1.3 mmol). The polymerization was carried out at room temperature. After 24 h of reaction, the crude mixture was dried under vacuum and the remaining solid was dissolved in MeOH (0.5 mL) and then precipitated in 10 mL of Et₂O unless otherwise stated. Centrifugation was applied when necessary to recover the precipitate. The polymers were analyzed by NMR in deuterated DMSO and SEC in DMF/LiBr.

Synthesis of poly(peptide-*alt*-peptoids) P₁-P₁₀ via Ugi-4C polymerization

In all experiments, the corresponding amino acid (4 mmol) was dissolved in 2.48 mL of Milli-Q water/MeOH (1:1 v:v) or MeOH. Aldehyde (5.2 mmol) was added to the stirred solution at room temperature followed by addition of isocyanide (5.2 mmol). The polymerization was carried out at room temperature. After 24 h of reaction, the crude mixture was dried

under vacuum and the remaining solid was dissolved in MeOH (10 mL) and then dialyzed against MeOH (cut-off 1 kDa) for 24 h except for P₇ and P₈ for which the dialysis was performed in DMF. The collected polymers (see Table S2†) were analyzed by SEC in DMF/LiBr with polystyrene calibration, NMR (¹H, HSQC, COSY, HMBC) (30 mg mL⁻¹ of deuterated DMSO), ATR, TGA and DSC.

Titration of P₅

The polymer solution (0.05 M) was prepared by solubilization of 272.6 mg of P₅ in 15 mL of HCl solution (0.1 M). A solution of sodium hydroxide was prepared by solubilizing 1 g in 250 mL Milli-Q water and calibrated with oxalic acid dihydrate in the presence of phenolphthalein. The NaOH concentration was 0.1019 M. The pH was monitored with a pH meter after each addition of 0.5 or 0.2 mL of NaOH solution in 10 mL of the polymer solution.

Cell viability

Solutions containing the polymers P₁, P₂, P₁₀ and PEG_{5k} were prepared at the desired concentrations (1000, 500 and 100 μg mL⁻¹ of DMEM) under aseptic conditions by filtration through a 0.2 μm filter and kept at 6 °C. HeLa cells were seeded in 96-well plates at a density of 2000 cells per well. The cells were incubated in DMEM at 37 °C under 5% CO₂. After 24 h, fresh media containing the polymers were added to the corresponding wells after removing the old media. Each condition was replicated in five wells. On the same plate, we prepared 5 controls which contain no polymers as well as 5 blanks that contain no cell or polymer. After incubation for 72 h at 37 °C under 5% CO₂, the wells were washed three times with DMEM-F12 and cell viability was measured by the MTS method. Cell viability was expressed as a percentage relative to the controls set at 100%. The experiment was repeated two more times. The final results are given by the averages of each measurement which are normalized for each plate using the average of the controls set at 100%. The standard deviations are represented by error bars after removal of outliers.

Results and discussion

Synthesis of polypeptoids

In a combinatorial approach, four amino acid building blocks were reacted with different aldehydes and isocyanides to design structurally diverse polypeptoids *via* Ugi-4C step-growth polymerization (Scheme 1D). In particular, we selected a series of amino acids in which the distance between the amine and the carboxylic acid moiety is sufficient to prevent 6-membered ring cyclisation *via* the intramolecular side reaction discussed above. In addition to glycylglycine (*glygly*), we considered another natural dipeptide of β-alanine and histidine, namely *carnosine*, notably because of its protonability and potential as precursors of pH-responsive materials. Two aliphatic and commercially available amino acids, *i.e.* γ-aminobutyric acid (*aba*)

and its hydroxylated derivative, 4-amino-3-hydroxybutyric acid (*haba*), completed the study.

First, these four amino acid building blocks were reacted with *tert*-butyl isocyanide (*t*BuNC) and formaldehyde (Table 1) in order to vary the structure of the backbone of the polypeptoids while keeping constant the nature of their side chains. Since step-growth polymerization *via* the Ugi-4CR is often carried out in MeOH,^{24,38,45} this solvent was selected for our first polymerization assays. All reactions were performed for 24 h at room temperature (RT) under an ambient atmosphere using an amino acid concentration of 1.6 M and a slight excess (1.3 eq.) of monofunctional reagents, *i.e.* *t*BuNC and formaldehyde. As demonstrated elsewhere,^{38,46} an excess of monofunctional components guarantees the availability of these reactants even at high conversions without a detrimental effect on the conversion. The four amino acids were insoluble in MeOH, certainly due to the stable zwitterionic form adopted by amino acids (Fig. S2†) at neutral pH, and the initial polymerization media consisted of a suspension. Along the reaction, the suspension became soluble in the cases of *glygly* and γ-aminobutyric acid while the products containing *carnosine* and 4-amino-3-hydroxybutyric acid remained in suspension. At the end of the reactions, products were collected by precipitation in diethyl ether (Et₂O) and analyzed by size exclusion chromatography (SEC) in DMF. The macromolecular parameters are presented in Table 1. Under these conditions, the formation of polymers with quite low molar masses was

Table 1 Ugi-4C polymerization of amino acid derivatives with *t*BuNC and formaldehyde

Entry	H ₂ N-R-CO ₂ H	Solvent	M _n ^a (g mol ⁻¹)	M _p ^a (g mol ⁻¹)	D ^a
1		MeOH	3300	4700	1.6
2		H ₂ O	4600	8100	1.8
3		H ₂ O/MeOH	5400	11 800	2.1
4		MeOH	1500	1500	1.2
5		H ₂ O	500	600	1.1
6		H ₂ O/MeOH	700	1000	1.5
7		MeOH	2400	3100	1.3
8		H ₂ O	3400	4300	1.4
9		H ₂ O/MeOH	5400	8400	1.6
10		MeOH	2700	3400	1.4
11		H ₂ O	4200	5400	1.9
12		H ₂ O/MeOH	4400	6900	1.7

Room temperature polymerization, [H₂N-R-CO₂H]/[formaldehyde]/[*t*BuNC] = 1/1.3/1.3. ^a Determined by SEC in DMF using PS calibration.

observed in all cases. Concerning the dipeptides, *glygly* gave a polypeptoid with an apparent average molar mass (M_n) of 3300 g mol^{-1} (entry 1, Table 1) whereas oligomers with M_n of about 1500 g mol^{-1} were formed with *carnosine* (entry 4, Table 1). On the other hand, the aliphatic *aba* and *haba* led to polymers with M_n of 2400 and 2700 g mol^{-1} respectively (entries 7 and 10, Table 1).

In order to tackle the solubility issues of the starting materials and to possibly increase of the molar mass of the polymers, we carried out the same reactions in water which is known as a suitable solvent for the Ugi-4CR.⁵⁰ As anticipated, the four amino acids were soluble in water and polymerizations started in the form of homogeneous solutions. Except for the *carnosine*-based experiment, we observed the precipitation of the polymers during the reaction. Overall, using water as a solvent in place of MeOH increased the apparent M_n for all polymerizations of amino acids except *carnosine* (entries 2, 5, 8 and 11, Table 1). Since amino acids are soluble in water and insoluble in MeOH and because the opposite trend is observed for the final products, we presumed that a mixture of both solvents (1 : 1 v : v) would ensure partial solubility of the amino acids while keeping the polymers soluble during the polymerization, which might be helpful to increase the molar masses. Except for *carnosine*, the results confirmed our hypothesis. Indeed, M_n values were higher in the MeOH/H₂O mixture than in pure solvents for *glygly*, *aba* and *haba* (entries 3, 9 and 12, Table 1). The improvement is even more striking when comparing the peak molar mass (M_p) which doubled when using a MeOH/H₂O mixture instead of MeOH as the solvent. Water afforded intermediate M_n and M_p for these polymers. However, using a mixture of solvents did not further improve the molar mass of the *carnosine*-based polypeptoid obtained in MeOH (1500 g mol^{-1}).

Besides the solvent, other parameters such as temperature, reaction time and stoichiometry of the reagents were varied in order to optimize the reaction and to possibly increase the molar mass of the polypeptoids (Table S1†). As illustrated for the Ugi-4C polymerization of *glygly*, increasing the temperature from 20 °C to 50 °C had a detrimental effect on the molar mass (compare entries 1 and 2 in Table S1†). Moreover, prolonging the reaction time from 24 to 120 h did not improve the molecular weight (compare entries 1 and 3 in Table S1†). Finally, polypeptoids produced from a stoichiometric amount of reagents had significantly lower M_n than those synthesized with 1.3 eq. of *t*BuNC and formaldehyde (1400 and 5400 g mol^{-1} respectively, entries 1 and 4 in Table S1†), which emphasized the benefit of using a slight excess of monofunctional reagents in the Ugi-4C polymerization of amino acid derivatives.

In order to gain insight into the reaction and the polymer structure, the *glygly*-based polypeptoid (entry 3, Table 1) was analyzed by MALDI-ToF (Fig. S3†). The MS spectrum showed different populations whose peaks are separated by an interval of 227.13 mass units corresponding to the expected repeating unit. Note that the intensity of the peaks significantly decreased with the molecular weight of the species due to the overestimation of low molecular weight ions.⁵¹ The intense

population at low m/z (e.g. $m/z = n \times 227.13 + 22.99$, m/z 704.32 ($n = 3$), m/z 931.43 ($n = 4$),...) was attributed to the sodiated macrocyclic compounds. Besides macrocycles, magnification at higher m/z values highlighted the presence of linear polymers with a large diversity of chain-ends which emphasizes the great complexity of the termination modes. Unfortunately, at this stage, these populations could not be unambiguously assigned and do not correspond to the most obvious terminal groups such as amine, carboxylic acid, imine, etc.

After this first screening, the synthesis of polymers with a decent molar mass, i.e. M_p above 3000 g mol^{-1} , was scaled up in order to characterize their structures and properties. For this purpose, the optimized polymerization conditions were used and polypeptoids were purified by dialysis instead of precipitation which was more efficient to remove residual traces of starting materials. The macromolecular parameters of the scaled-up polymers P₁, P₂ and P₃ prepared from *glygly*, *aba* and *haba*, respectively, are presented in Table S2.† Their SEC analyses are shown in Fig. S4† after purification. ¹H NMR analyses performed in DMSO-d₆ confirmed the chemical structures of P₁₋₃ (Fig. 1). The three polymers present typical signals of the α -amido amide motif generated by the Ugi-4C reaction, i.e. the amidic protons **a** around 7.5 ppm, the methylene protons **b** around 3.9 ppm and the methyl protons **c** of the *tert*-butyl group at 1.3 ppm (Fig. 1). 2D NMR experiments (COSY and HSQC) confirmed these assignments and helped to attribute other protons specific to the amino acids (Fig. S5†). Infrared analyses emphasized the presence of amides with characteristic peaks at 1645 and 1540 cm^{-1} corresponding to C=O stretching and N-H deformation, respectively, whereas the aliphatic part of the polymers was evidenced by CH₃ deformation

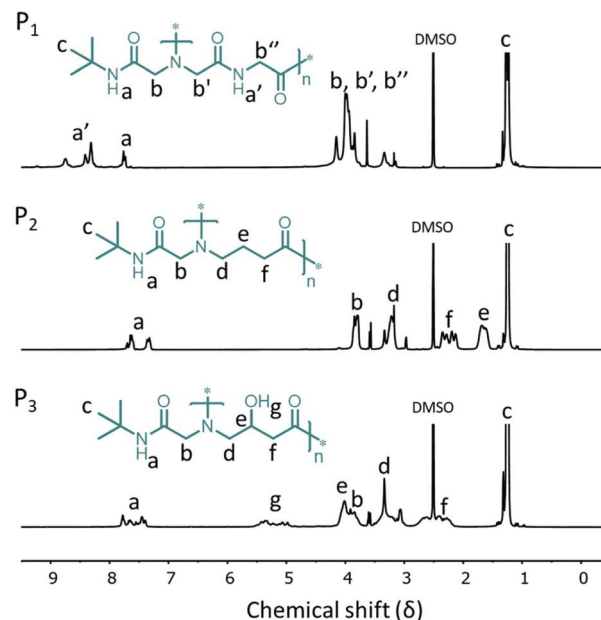


Fig. 1 ¹H NMR spectra of P₁, P₂ and P₃ in DMSO-d₆.

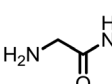
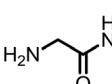
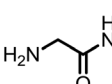
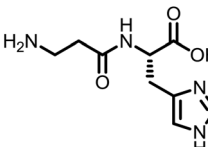
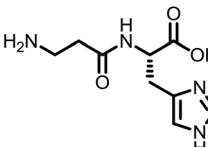
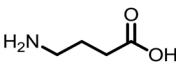
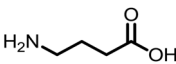
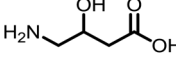
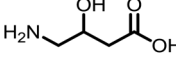
and CH₂ scissoring peaks between 1460 and 1390 cm⁻¹ (Fig. S6†).

Next, the polymerization of the four amino acids with *t*BuNC was investigated with another aldehyde, *i.e.* isobutyraldehyde (Table 2). H₂O, MeOH and a mixture of both were considered for the polymerization of *glygly* involving isobutyraldehyde. In spite of a minor secondary peak at 1000 g mol⁻¹, the best results were obtained in MeOH with *M_p* and *M_n* equal to 12 400 and 5300 g mol⁻¹, respectively (entry 3, Table 2). Trials carried out in water and in water/MeOH gave lower *M_n* values, *i.e.* 2100 and 2600 g mol⁻¹ respectively (entries 1 and 2, Table 2), and the SEC chromatogram showed a broad and multimodal peak for the polymerization in water (Fig. S7†). The MALDI-TOF analysis of this polypeptoid (entry 3, Table 2) confirmed the nature of the repeating unit (269.17 mass units) and the presence of low molecular weight macrocyclic species (Fig. S8†). The other three amino acids were reacted with *t*BuNC and isobutyraldehyde in the most promising solvents, *i.e.* MeOH and the MeOH/H₂O mixture. In all the cases, the macromolecular parameters of the polymers were quite similar in both solvents. Note that *carnosine* gave slightly higher *M_n* in MeOH/H₂O (3300 g mol⁻¹, entry 4, Table 2) compared to MeOH due to lower contamination by low molar mass oligomers. *Aba* led to polymers with slightly higher *M_n* and *M_p* in MeOH (entry 7, Table 2) while *haba* only produced low molar mass polymers with the *M_p* below the threshold of 3000 g mol⁻¹. After this second screening, the synthesis of three more

polypeptoids (Table 2, entries 3, 4 and 7, respectively) was deemed worthy for scaling up (*P₄₋₆* in Table S2†). The structures of *P₄₋₆* were corroborated by ¹H NMR (Fig. 2) and 2D NMR (COSY and HSQC, Fig. S9†) and also by IR analyses, showing characteristic peaks of C=O stretching and N-H deformation of amides at 1645 and 1540 cm⁻¹, respectively (Fig. S10†).

Eventually, a series of isocyanides were tested with both aldehydes in the Ugi-4CP of *glygly*. In addition to *t*BuNC, two aliphatic isocyanides with different lengths and branchings, namely cyclohexyl and *n*-pentyl isocyanide, were reacted for 24 h in water or methanol with *glygly* in the presence of formaldehyde or isobutyraldehyde (entries 1–3 and 6–8, Table 3). Regardless of the solvent used, we observed a significant decrease of the *M_n* of the polymer when *t*BuNC was replaced by cyclohexyl (from 5300 g mol⁻¹ to 3600 g mol⁻¹ in MeOH). The drop in the *M_n* was even more pronounced for *n*-pentyl isocyanide (2300 g mol⁻¹, entry 6, Table 3). Such a trend suggests that the efficiency of the present Ugi-4CR depends on the bulkiness of the isocyanides. The latter can be estimated by the Charton values (*v*) of the substituents (*v_{tert-butyl}* = 1.24, *v_{c-hexyl}* = 0.87, *v_{n-pentyl}* = 0.68) derived from van der Waals radii.^{52,53} In these studies, the kinetics of various reactions were found to be directly related to the bulkiness of the reagents: the more bulkier the substituent, the slower the reaction.^{52,53} Therefore, the steric hindrance of the isocyanide could have affected the kinetics of concurrent reactions

Table 2 Ugi-4C polymerization of amino acids with *t*BuNC and isobutyraldehyde

Entry	H ₂ N-R-CO ₂ H	Solvent	<i>M_n</i> ^a (g mol ⁻¹)	<i>M_p</i> ^a (g mol ⁻¹)	<i>D</i> ^a
1		H ₂ O	2100	5100	1.7
2		H ₂ O/MeOH	2600	4100	1.6
3		MeOH ^b	5300	12 400/1000	2.2
4		H ₂ O/MeOH	3300	5300	1.6
5		MeOH	2700	6400/1100	1.9
6		H ₂ O/MeOH	1700	5200/1000	2.3
7		MeOH ^b	2400	5400	2.0
8		H ₂ O/MeOH ^b	2100	1900	1.3
9		MeOH ^b	1700	1900	1.2

Room temperature polymerization, [H₂N-R-CO₂H]/[isobutyraldehyde]/[*t*BuNC] = 1/1.3/1.3. ^a Determined by SEC in DMF using PS calibration. ^b Purified by precipitation in H₂O instead of Et₂O.

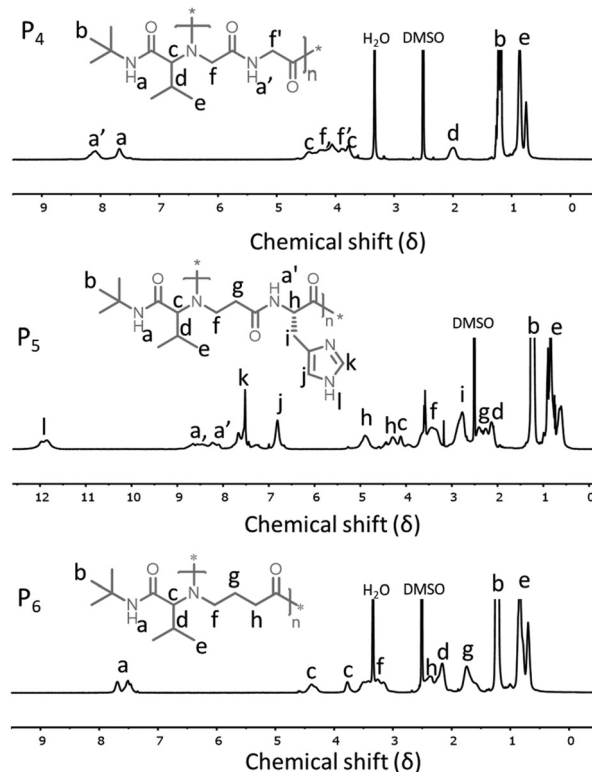



Fig. 2 ¹H NMR spectra of polypeptoids *P₄*, *P₅* and *P₆* in DMSO-*d*₆ (see Table S2† for details).

Table 3 Ugi-4C polymerization of *glygly* with different aldehydes and isocyanides


Entry	R ₁	R ₂	Solvent	M _n ^a (g mol ⁻¹)	M _p ^a (g mol ⁻¹)	D ^a
1	-H	- <i>t</i> Bu	H ₂ O	4600	8100	1.8
2	-H	-Cyclohexyl	H ₂ O	2100	3600	1.8
3	-H	-Pentyl	H ₂ O	1500	2400	2.0
4	-H	-CH ₂ CO ₂ Et	H ₂ O	700	700	1.5
5	-H	-C ₂ H ₄ (<i>N</i> -morpholino)	H ₂ O	600	800	1.3
6	-CH(CH ₃) ₂	- <i>t</i> Bu	MeOH ^b	5300	12 400/1000	2.5
7	-CH(CH ₃) ₂	-Cyclohexyl	MeOH	3600	5200	1.5
8	-CH(CH ₃) ₂	-Pentyl	MeOH ^b	2300	3100	1.5
9	-CH(CH ₃) ₂	-CH ₂ CO ₂ Et	MeOH ^b	1600	1800	1.2
10	-CH(CH ₃) ₂	-C ₂ H ₄ (<i>N</i> -morpholino)	MeOH	2400	3200	1.5

Room temperature polymerization, [*glygly*]/[R₁CHO]/[R₂NC] = 1/1.3/1.3. ^a Determined by SEC in DMF using PS calibration. ^b Purified by precipitation in H₂O instead of Et₂O.

more than the Ugi-4CP itself. This might explain why bulkier isocyanides (*t*Bu > cyclohexyl > *n*-pentyl) led to polypeptoids with higher molecular masses. Finally, two other isocyanides bearing an ester or a morpholino function, namely ethyl isocyanoacetate and 2-morpholinoethyl isocyanide, were tested. Oligomers were obtained (M_n of 700 and 600 g mol⁻¹) when the reaction was performed in water with formaldehyde (entries 4 and 5, Table 3) whereas their polymerization in MeOH with isobutyraldehyde gave higher M_n especially for 2-morpholinoethyl isocyanide ($M_n = 2400$ g mol⁻¹, $M_p = 3200$ g mol⁻¹) (entry 10, Table 3). Four novel polypeptoids (P₇₋₁₀, Table S2[†]) were scaled up (entries 2, 7, 8 and 10, Table 3) and characterized by NMR (Fig. S11 and S12[†]) and IR (Fig. S13[†]). Overall, a library of ten novel polypeptoids differing by the nature of their backbone and/or side chains was produced by Ugi-4CP highlighting the strength of this combinatorial MCR approach. Thereafter, the thermal and solution properties of these unique polymers were measured and put in perspective with their structural variations.

Thermal properties of polypeptoids

Polypeptoids P₁₋₁₀ present different backbones formed by the amino acids and various side chains composed of aldehydes and isocyanides, all articulated around a typical α -amido amide moiety generated by the Ugi-4CR. Such a systematic variation of the reactants allowed us to study the relationship between the structure of the polypeptoids and their thermal properties. All polymers were subjected to thermal gravimetric analysis (TGA) to determine their onset degradation temperature, that is, the temperature at 5 weight% of loss (T_{OD}) (Fig. S14[†]). Differential scanning calorimetry (DSC) analyses were also carried out to measure their glass transition temperatures (T_g) and their melting temperatures (T_m) (Fig. S15[†]). Although the thermal properties of polymers depend to a certain extent on their degree of polymerization, in this study,

we considered polymers with molar masses in the same range.

First, the thermal properties of P₁₋₃ having identical side chains with three different backbones made of *glygly*, *aba* and *haba* were compared (Fig. 3). The *aba*-based polymer P₂ with aliphatic carbons between the peptoid bonds showed the highest thermal stability with a T_{OD} value equal to 325 °C. Introduction of an additional peptide bond within the repeating unit of the polypeptoid, *i.e.* *glygly*-based polymer P₁, decreased the T_{OD} by 63 °C. The decrease of the onset degradation temperature was even greater for the *haba*-based polymer P₃ ($T_{OD} = 232$ °C) likely due to the elimination of the hydroxyl group similarly to the degradation of poly(vinylalcohol) (PVA).⁵⁴ This hypothesis is comforted by the degradation profile of P₃ showing a two-step degradation like PVA (Fig. S14[†]).⁵⁵ On the other hand, no T_m was detected in the DSC analyses of P₁₋₃ (Fig. S15[†]). Among them, P₂ presented the lowest T_g (93 °C) as a result of the relatively high flexibility of the aliphatic sections of the main chain. Interestingly, the presence of an alcohol in P₃ increased the T_g to 117 °C. In this case, the alcohol moieties probably induce extra intermolecular hydrogen bond interactions which reduce the chain mobility. Moreover, the formation of a six-membered ring *via* intramolecular H-bond between the alcohol and the adjacent tertiary amide can also rigidify the backbone (Fig. S16[†]). As anticipated, P₁ had the highest T_g (162 °C) among the three polymers. Indeed, the peptide bond within the repeating unit of P₁ certainly favors interchain interactions *via* H-bonding but also the formation of a five-membered ring *via* intramolecular hydrogen bond interaction between the secondary and tertiary amides, as shown in Fig. S16,† which stiffens the main chain.

The influence of the side chains, and thus of the choice of the aldehyde and isocyanide, on the thermal properties of the polypeptoids was then examined (Fig. 3). In this perspective, we considered three pairs of polymers (P₁-P₄, P₂-P₆ and P₇-P₈)

Influence of the backbone			Influence of the side-chain												
amino acids	T_g	T_{OD}	a) aldehydes	T_g	T_{OD}	b) isocyanides	T_g	T_{OD}							
	(°C)	(°C)		(°C)	(°C)		(°C)	(°C)	(°C)						
P ₁		162	262	P ₁		162	262	P ₄		169	259	P ₈		139	264
P ₂		93	325	P ₂		93	325	P ₉		98	251	P ₁₀		115	245
P ₃		117	232	P ₆		99	344								
				P ₇		146	244								
				P ₈		139	264								

Fig. 3 Comparison of the thermal properties of polypeptoids with various backbones and/or side chains.

which differ by the aldehyde used in their synthesis (*i.e.* formaldehyde or isobutyraldehyde). In each couple of polymers, the maximum variations in T_{OD} and T_g were smaller than 20 °C and 10 °C, respectively, highlighting the limited impact of this group on the thermal properties. On the other hand, polypeptoids produced from different isocyanides (P₄, P₈, P₉ and P₁₀) showed no differences regarding their T_{OD} meaning that their degradation mainly depends on the backbone structure. In contrast, the choice of the isocyanide precursor significantly affected the T_g . In the series of aliphatic isocyanides, the glass transition temperature of the resulting polypeptoids decreased in the following order: *tert*-butyl > cyclohexyl > *n*-pentyl ($T_{g, P4} > T_{g, P8} > T_{g, P9}$). In order to rationalize these observations, it is worth considering a recent study by Gomez *et al.*⁵⁶ demonstrating that the dynamics of the backbone and the side chain of a polymer, in that case polythiophene, are mutually affected. Briefly, an increase of the side chain mobility led to an increase of the backbone mobility and eventually to a decrease of T_g . The dynamics of an atom of the side chain was shown to increase with its distance from the backbone underlying the dependence of the mobility of the chains on the length of the alkyl side group. When comparing branched and linear alkyl chains with the same number of carbon atoms, the mobility of the former was lower since its carbons are located closer to the main chains. These conclusions were validated for polypeptoids with different side chain lengths.⁵⁷ In the light of these considerations, the lower T_g observed for P₉ compared to P₄, bearing an *n*-pentyl and *tert*-butyl group respectively, can be rationalized by the higher mobility of the *n*-pentyl group. The same reasoning applies to the higher T_g of P₈ bearing a cyclohexyl group compared to P₉ (*n*-pentyl) since atoms of cyclohexyl are closer to the main chain and the mobility of this group is restrained by its cyclic structure. A similar trend was reported for poly(methacrylate)s with *n*-pentyl and

cyclohexyl pending moieties and supported by the free volume theory.⁵⁶ Eventually, the lower T_g of P₈ compared to P₄ can also be explained based on the distance between the atoms of the side chain and the backbone which is higher for the furthest methylene group of cyclohexyl compared to the methyl ends of *tert*-butyl. Note that P₁₀ with morpholino lateral groups exhibited a quite similar T_{OD} (251 °C) and intermediate T_g (115 °C) in comparison with their aliphatic counterparts.

Solution behavior

Polymers that respond to stimuli such as changes of temperature or external pH are steadily gaining increasing interest for advanced applications especially in the biomedical field.^{58–60} In this context, the aqueous solution behavior of our library of polypeptoids P_{1–10} was examined under different conditions. A first screening showed that five polypeptoids are soluble in water at a concentration of 2 mg mL⁻¹. These include P_{1–3}, all produced from formaldehyde. In contrast, the corresponding polymers obtained from isobutyraldehyde were insoluble probably due to the higher hydrophobicity and bulkiness of the lateral chain. The sole exceptions were polypeptoids P₁₀ and P₅ which possess polar morpholino and imidazole pending groups. Note that P₁₀ was soluble in water in the whole range of pH while the solubilization of the *carnosine*-based polymer P₅ required an acidic medium as discussed below.

The polypeptoid P₅ exhibited a pH-responsive behavior and solubilized in water after protonation of the pendant imidazole of the histidine units. The pK_a of P₅, measured by basic titration of an acidified solution of P₅, was found to be equal to 5.9 (Fig. 4A).

During the titration, the precipitation of P₅ began at pH 5.8, so close to the measured pK_a . This behavior was very similar to that of poly-L-histidine which is soluble below pH 6 near its pK_a . Interestingly, the sudden pH rise suggests that the proton-

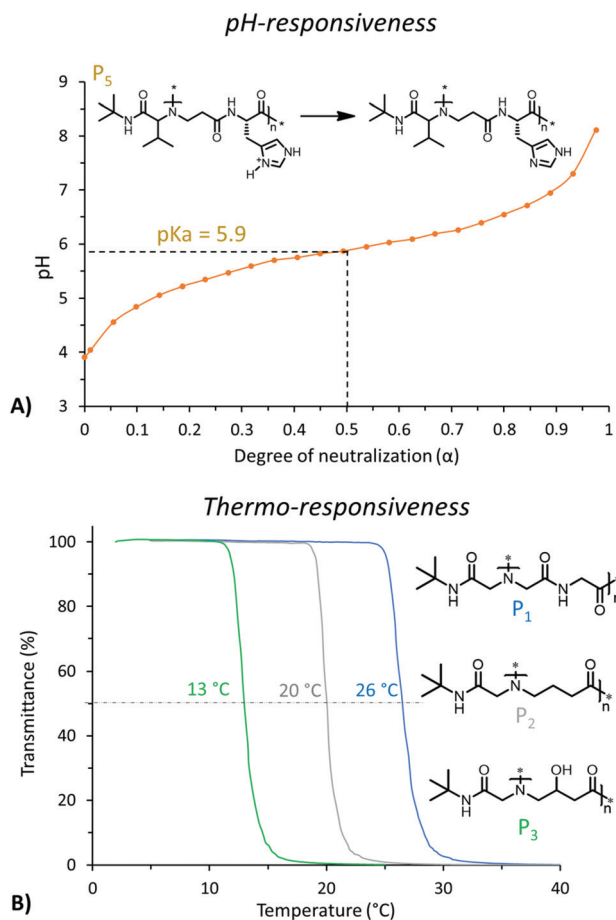


Fig. 4 (A) pH vs. the degree of neutralization for titrations of *carnosine* and P_5 with NaOH. (B) Transmittance vs. temperature for turbidimetry measurements of aqueous solution of P_1 , P_2 and P_3 at a concentration of 2 mg mL^{-1} .

ability of the histidine side chain does not depend on neighboring interactions. It was confirmed by the Henderson-Hasselbalch equation (eqn (1)).⁶¹

$$\text{pH} = \text{p}K_a - m \log\left(\frac{1 - \alpha}{\alpha}\right) \quad (1)$$

where α corresponds to the degree of neutralization, K_a is the average dissociation constant and the parameter m reflects the electrostatic interaction between neighbor ionizable groups.

In practice, the m value of P_5 was extracted from the slope of Henderson-Hasselbalch plots in a region where the α value ranges between 0.2 and 0.6 (Fig. S17†). It was equal to 1 showing the absence of neighboring interactions within P_5 . By comparison, the m value of poly(vinylamine)s having a high density of amine functions is around 5.3.⁶²

The possible thermo-responsiveness of the polypeptoids P_1 , P_2 , P_3 , P_5 and P_{10} was also explored. The starting polymer solutions (2 mg mL^{-1}) were prepared at low temperature ($6 \text{ }^\circ\text{C}$) and neutral pH, except for P_5 which was dissolved in 60 mM HCl to ensure its solubility. The thermal response of the polypeptoid

solutions was studied by monitoring the evolution of their transmittance at 260 nm during heating and cooling cycles. The cloud point temperature (T_{CP}), that is the temperature above which a demixing of phases occurs, was measured at 50% loss of transmittance. Concerning P_5 and P_{10} , no thermo-responsive behavior was observed upon heating the polymer solutions (2 mg mL^{-1}) until $90 \text{ }^\circ\text{C}$. In these cases, the imidazolium and morpholino group drastically enhanced the solubility of the polypeptoids preventing their solution demixing. As an additional proof of their improved solubility, more than 50 mg of P_5 and P_{10} were dissolved per mL of water. In contrast, the *glygly*-based polypeptoid P_1 exhibited a T_{CP} value of $26.5 \text{ }^\circ\text{C}$ upon heating, in perfect accordance with previous observations (Fig. 4B).⁴⁶ The reversibility of the transition was attested by monitoring the transmittance during the cooling (Fig. S18†). In this case, a hysteresis phenomenon of a few degrees was observed suggesting the formation of intermolecular hydrogen bonds in the collapsed state *via* the secondary amides, as was the case for poly(*N*-isopropylacrylamide).⁶³ Expectedly, the corresponding *aba*-based polypeptoid P_2 showed a lower T_{CP} value ($20 \text{ }^\circ\text{C}$) compared to P_1 due to the increase of the hydrophobicity of the backbone resulting from the substitution of a secondary amide for an aliphatic chain (Fig. 4B). More surprisingly, the introduction of a polar hydroxyl group within the aminobutyric acid backbone P_3 further decreased the T_{CP} to $13 \text{ }^\circ\text{C}$ suggesting that the $-\text{OH}$ groups are preferentially involved in inter- or intra-chain interactions rather than in the solvation of the polymer. All in all, we identified three thermo-responsive polypeptoids with specific transition temperatures.

Cell viability

As a first evaluation of the potential of these novel polypeptoid sequences in the biomedical field, we assessed their cytotoxicity towards HeLa cells *via* MTS assay. In this study, we considered polymers that are soluble at $37 \text{ }^\circ\text{C}$ in the cell culture medium at certain concentrations ranging from

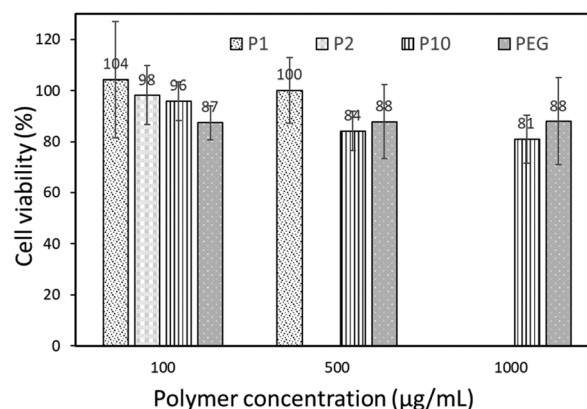


Fig. 5 Cell viability of P_1 , P_2 and P_{10} compared with PEG_{5k} evaluated by the MTS method after 72 h of incubation with HeLa cells at $37 \text{ }^\circ\text{C}$. The error bars represent the standard deviations.

100–1000 $\mu\text{g mL}^{-1}$, namely P_1 , P_2 and P_{10} . More precisely, clear solutions of P_1 and P_2 could be prepared for concentrations of 500 $\mu\text{g mL}^{-1}$ and 100 $\mu\text{g mL}^{-1}$, respectively, and the morpholino-functional P_{10} was soluble at all concentrations. In addition to our polypeptoids, poly(ethylene glycol) (PEG) (5000 g mol^{-1}) was selected as a common standard.^{24,64} In practice, cells were incubated at 37 °C for 72 hours with the polymer and cell viability was expressed as a percentage relative to the controls containing no polymers set at 100%. The data are presented in Fig. 5. The PEG standard logically exhibited low cytotoxicity towards HeLa cells with a minimal viability of 88% at 1000 $\mu\text{g mL}^{-1}$. Importantly, the *glygly*-based P_1 and P_{10} as well as the *aba*-containing P_2 showed excellent cell viability levels that were statistically similar to those of PEG. A cell viability slightly higher than 100% was measured for P_1 due to statistical error. Interestingly, for the morpholino-functional P_{10} , we noticed a slight increase of the toxicity with the increase of its concentration but its intrinsic cell viability remained competitive to PEG even at the highest concentration. This dependence of cell viability on the concentration of P_{10} was confirmed by a one-way ANOVA test (Fig. S19†). Overall, the data clearly demonstrated the low toxicity of these polypeptoid sequences obtained by this single-step MCP without advanced purification.

Conclusions

In summary, we developed a straightforward one-step synthesis of polypeptoid analogues *via* Ugi-4C polymerization of amino acid derivatives. In a combinatorial approach, a wide variety of reactants, namely amino acids, aldehydes and isocyanides, were considered in this multicomponent polymerization with the aim to prepare a library of structurally diverse polypeptoids. The polymerization conditions were optimized and scaled up for ten unprecedented polymers. The systematic variation of the three constituents of the reaction allowed us to study the influence of a change in the backbone or in the side chain on the thermal and solution properties of the polypeptoids. It notably revealed that the T_g of the polypeptoids markedly depends on the choice of the amino acid and of the isocyanide while changing the aldehyde has little impact on their thermal properties. In contrast, the replacement of formaldehyde for isobutyraldehyde strongly affects the water solubility of the polymer. In this respect, we highlighted the excellent water solubility of the morpholino-functionalized P_{10} , the pH-responsiveness of the *carnosine*-based P_5 and the thermo-responsiveness of a series of polypeptoids P_{1-3} with various transition temperatures. The low cytotoxicity of some polypeptoid structures was also demonstrated. Considering the ease of this multicomponent polymerization, the great variety of potential substrates and the valuable properties of the polymers prepared accordingly, this approach is attractive to sustain the demand for innovative polypeptoid analogues and the applications resulting therefrom.

Conflicts of interest

There are no conflicts to declare.

Acknowledgements

The authors are grateful to the Belgian National Fund for Scientific Research (F.R.S.-FNRS) in Belgium for the financial support. P. Stiernet and A. Debuigne are FNRS Research Fellow and FNRS Senior Research Associate, respectively. The authors also thank P. Matagne (ULiege) for providing the spectrophotometers for the turbidimetry analyses.

Notes and references

- R. Luxenhofer, C. Fetsch and A. Grossmann, *J. Polym. Sci., Part A: Polym. Chem.*, 2013, **51**, 2731–2752.
- C. Secker, S. M. Brosnan, R. Luxenhofer and H. Schlaad, *Macromol. Biosci.*, 2015, **15**, 881–891.
- J. M. Matharage, J. D. Minna, R. A. Brekken and D. G. Udugamasooriya, *ACS Chem. Biol.*, 2015, **10**, 2891–2899.
- R. D. Jahnsen, N. Frimodt-Møller and H. Franzyk, *J. Med. Chem.*, 2012, **55**, 7253–7261.
- D. R. Buckle, P. W. Erhardt, C. R. Ganellin, T. Kobayashi, T. J. Perun, J. Proudfoot and J. Senn-Bilfinger, *Pure Appl. Chem.*, 2013, **85**, 1725–1758.
- O. Roy, C. Caumes, Y. Esvan, C. Didierjean, S. Faure and C. Taillefumier, *Org. Lett.*, 2013, **15**, 2246–2249.
- J. S. Laursen, J. Engel-Andreasen and C. A. Olsen, *Acc. Chem. Res.*, 2015, **48**, 2696–2704.
- B.-C. Lee, R. N. Zuckermann and K. A. Dill, *J. Am. Chem. Soc.*, 2005, **127**, 10999–11009.
- A. M. Rosales, H. K. Murnen, S. R. Kline, R. N. Zuckermann and R. A. Segalman, *Soft Matter*, 2012, **8**, 3673–3680.
- K. Kirshenbaum, A. E. Barron, R. A. Goldsmith, P. Armand, E. K. Bradley, K. T. V. Truong, K. A. Dill, F. E. Cohen and R. N. Zuckermann, *Proc. Natl. Acad. Sci. U. S. A.*, 1998, **95**, 4303–4308.
- P. Armand, K. Kirshenbaum, R. A. Goldsmith, S. Farr-Jones, A. E. Barron, K. T. V. Truong, K. A. Dill, D. F. Mierke, F. E. Cohen, R. N. Zuckermann and E. K. Bradley, *Proc. Natl. Acad. Sci. U. S. A.*, 1998, **95**, 4309–4314.
- M. Goodman, F. Chen and F. R. Prince, *Biopolymers*, 1973, **12**, 2549–2561.
- S. B. Y. Shin, B. Yoo, L. J. Todaro and K. Kirshenbaum, *J. Am. Chem. Soc.*, 2007, **129**, 3218–3225.
- J. K. Pokorski, L. M. Miller Jenkins, H. Feng, S. R. Durell, Y. Bai and D. H. Appella, *Org. Lett.*, 2007, **9**, 2381–2383.
- D. J. Gordon, K. L. Sciarretta and S. C. Meredith, *Biochemistry*, 2001, **40**, 8237–8245.
- C. Fetsch, A. Grossmann, L. Holz, J. F. Nawroth and R. Luxenhofer, *Macromolecules*, 2011, **44**, 6746–6758.

- 17 S. Lin, B. Zhang, M. J. Skoumal, B. Ramunno, X. Li, C. Wesdemiotis, L. Liu and L. Jia, *Biomacromolecules*, 2011, **12**, 2573–2582.
- 18 N. J. Brown, M. T. Dohm, J. Bernardino de la Serna and A. E. Barron, *Biophys. J.*, 2011, **101**, 1076–1085.
- 19 S. M. Miller, R. J. Simon, S. Ng, R. N. Zuckermann, J. M. Kerr and W. H. Moos, *Drug Dev. Res.*, 1995, **35**, 20–32.
- 20 B. J. Bruno, G. D. Miller and C. S. Lim, *Ther. Delivery*, 2013, **4**, 1443–1467.
- 21 J. H. Hamman, G. M. Enslin and A. F. Kotzé, *BioDrugs*, 2005, **19**, 165–177.
- 22 S. Frokjaer and D. E. Otzen, *Nat. Rev. Drug Discovery*, 2005, **4**, 298–306.
- 23 S. H. Lahasky, X. Hu and D. Zhang, *ACS Macro Lett.*, 2012, **1**, 580–584.
- 24 Y. Tao, S. Wang, X. Zhang, Z. Wang, Y. Tao and X. Wang, *Biomacromolecules*, 2018, **19**, 936–942.
- 25 J. Sun and R. N. Zuckermann, *ACS Nano*, 2013, **7**, 4715–4732.
- 26 D. Zhang, S. H. Lahasky, L. Guo, C.-U. Lee and M. Lavan, *Macromolecules*, 2012, **45**, 5833–5841.
- 27 A. S. Knight, E. Y. Zhou, M. B. Francis and R. N. Zuckermann, *Adv. Mater.*, 2015, **27**, 5665–5691.
- 28 J. A. W. Kruijtzter, L. J. F. Hofmeyer, W. Heerma, C. Versluis and R. M. J. Liskamp, *Chem. – Eur. J.*, 1998, **4**, 1570–1580.
- 29 R. J. Simon, R. S. Kania, R. N. Zuckermann, V. D. Huebner, D. A. Jewell, S. Banville, S. Ng, L. Wang, S. Rosenberg and C. K. Marlowe, *Proc. Natl. Acad. Sci. U. S. A.*, 1992, **89**, 9367–9371.
- 30 Y. Gao and T. Kodadek, *Chem. Biol.*, 2013, **20**, 360–369.
- 31 R. N. Zuckermann, J. M. Kerr, S. B. H. Kent and W. H. Moos, *J. Am. Chem. Soc.*, 1992, **114**, 10646–10647.
- 32 N. Gangloff, C. Fetsch and R. Luxenhofer, *Macromol. Rapid Commun.*, 2013, **34**, 997–1001.
- 33 N. Gangloff, J. Ulbricht, T. Lorson, H. Schlaad and R. Luxenhofer, *Chem. Rev.*, 2016, **116**, 1753–1802.
- 34 A. Grossmann and R. Luxenhofer, *Macromol. Rapid Commun.*, 2012, **33**, 1714–1719.
- 35 J. Chai, G. Liu, K. Chaicharoen, C. Wesdemiotis and L. Jia, *Macromolecules*, 2008, **41**, 8980–8985.
- 36 S. Marcaccini and T. Torroba, *Nat. Protoc.*, 2007, **2**, 632–639.
- 37 G. A. Medeiros, W. A. da Silva, G. A. Bataglion, D. A. C. Ferreira, H. C. B. de Oliveira, M. N. Eberlin and B. A. D. Neto, *Chem. Commun.*, 2014, **50**, 338–340.
- 38 A. Sehlinger, P. K. Dannecker, O. Kreye and M. A. R. Meier, *Macromolecules*, 2014, **47**, 2774–2783.
- 39 R. Kakuchi, *Angew. Chem., Int. Ed.*, 2014, **53**, 46–48.
- 40 N. Gangloff, D. Nahm, L. Döring, D. Kuckling and R. Luxenhofer, *J. Polym. Sci., Part A: Polym. Chem.*, 2015, **53**, 1680–1686.
- 41 P. Stiernet, P. Lecomte, J. De Winter and A. Debuigne, *ACS Macro Lett.*, 2019, **8**, 427–434.
- 42 Y. Tao, Z. Wang and Y. Tao, *Biopolymers*, 2019, **110**, e23288.
- 43 S. Wang, Y. Tao, J. Wang, Y. Tao and X. Wang, *Chem. Sci.*, 2019, **10**, 1531–1538.
- 44 M. Hartweg, C. J. C. Edwards-Gayle, E. Radvar, D. Collis, M. Reza, M. Kaupp, J. Steinkoenig, J. Ruokolainen, R. Rambo, C. Barner-Kowollik, I. W. Hamley, H. S. Azevedo and C. R. Becer, *Polym. Chem.*, 2018, **9**, 482–489.
- 45 X. Zhang, S. Wang, J. Liu, Z. Xie, S. Luan, C. Xiao, Y. Tao and X. Wang, *ACS Macro Lett.*, 2016, **5**, 1049–1054.
- 46 A. Al Samad, J. De Winter, P. Gerbaux, C. Jérôme and A. Debuigne, *Chem. Commun.*, 2017, **53**, 12240–12243.
- 47 Y. Koyama and P. G. Gudeangadi, *Chem. Commun.*, 2017, **53**, 3846–3849.
- 48 Y. Koyama, A. B. Ihsan, T. Taira and T. Imura, *RSC Adv.*, 2018, **8**, 7509–7513.
- 49 A. Bin Ihsan, M. Taniguchi and Y. Koyama, *Macromol. Rapid Commun.*, 2020, 2000480.
- 50 M. C. Pirrung and K. Das Sarma, *J. Am. Chem. Soc.*, 2004, **126**, 444–445.
- 51 P. M. Lloyd, K. G. Suddaby, J. E. Varney, E. Scrivener, P. J. Derrick and D. M. Haddleton, *Eur. Mass Spectrom.*, 1995, **1**, 293–300.
- 52 M. Charton, *J. Am. Chem. Soc.*, 1975, **97**, 1552–1556.
- 53 D. P. Gavin and J. C. Stephens, *ARKIVOC*, 2011, **2011**, 407–421.
- 54 P. Alexy, D. Bakoš, G. Crkoňová, K. Kolomaznik and M. Kršiak, *Macromol. Symp.*, 2001, **170**, 41–50.
- 55 Z. Peng and L. X. Kong, *Polym. Degrad. Stab.*, 2007, **92**, 1061–1071.
- 56 P. Zhan, W. Zhang, I. E. Jacobs, D. M. Nisson, R. Xie, A. R. Weissen, R. H. Colby, A. J. Moulé, S. T. Milner, J. K. Maranas and E. D. Gomez, *J. Polym. Sci., Part B: Polym. Phys.*, 2018, **56**, 1193–1202.
- 57 C. Fetsch and R. Luxenhofer, *Polymer*, 2013, **5**, 112–127.
- 58 M. Sponchioni, U. Capasso Palmiero and D. Moscatelli, *Mater. Sci. Eng., C*, 2019, **102**, 589–605.
- 59 Y. Shen, X. Fu, W. Fu and Z. Li, *Chem. Soc. Rev.*, 2015, **44**, 612–622.
- 60 K.-S. Krannig and H. Schlaad, *J. Am. Chem. Soc.*, 2012, **134**, 18542–18545.
- 61 E. S. Lee, H. J. Shin, K. Na and Y. H. Bae, *J. Controlled Release*, 2003, **90**, 363–374.
- 62 S. Kobayashi, K. Do Suh and Y. Shirokura, *Macromolecules*, 1989, **22**, 2363–2366.
- 63 H. Cheng, L. Shen and C. Wu, *Macromolecules*, 2006, **39**, 2325–2329.
- 64 J. Zhang, M. Zhang, F. Du and Z. Li, *Macromolecules*, 2016, **49**, 2592–2600.